IntersectX: An Efficient Accelerator for Graph Mining

Gengyu Rao[1], Jingji Chen[1], Jason Yik[1], and Xuehai Qian[1]

[1]University of Southern California, Los Angeles, CA

Abstract—Graph pattern mining applications try to find all embeddings that match specific patterns. Compared to the traditional graph computation, graph mining applications are computation-intensive. The state-of-the-art method, *pattern enumeration*, constructs the embeddings that match the pattern. The key operation—*intersection*—of two edge lists, poses challenges to conventional architectures and requires substantial execution time.

In this paper, we propose *IntersectX*, a *vertically* designed accelerator for pattern enumeration with stream instruction set extension and architectural supports based on *conventional* processor. The stream based ISA can be considered as a natural extension to the traditional instructions that operate on scalar values. We develop the IntersectX architecture composed of specialized mechanisms that efficiently implement the stream ISA extensions, including: (1) Stream Mapping Table (SMT) that records the mapping between stream ID and stream register; (2) the read-only Stream Cache (S-Cache) that enables efficient stream data movements; (3) tracking the dependency between streams with a property of intersection; (4) Stream Value Processing Unit (SVPU) that implements sparse value computations; and (5) the nested intersection translator that generates micro-op sequences for implementing nested intersections. We implement IntersectX ISA and architecture on zSim, and test it with seven popular graph mining applications (triangle/three-chain/tailed-traingle counting, 3-motif mining, 4/5-clique counting, and FSM) on ten real graphs. We develop our own implementation of AutoMine (InHouseAutomine) [1]. The results show that IntersectX significantly outperforms InHouseAutomine on CPU, on average 10.7× and up to 83.9×; and GRAMER, a state-of-the-art graph pattern mining accelerator, based on exhaustive check, on average 40.1× and up to 181.8×.

I. INTRODUCTION

Graph processing, which attempts to extract the underlying unstructured information of massive graph data, has attracted significant attention in the recent decade [15], [47], [51], [58]. Graph computation and graph pattern mining (GPM) are two major workloads of graph processing [57]. Different from the traditional iterative graph computation (e.g., PageRank, BFS, SSSP, etc.) with simple computations, GPM applications are *computation-intensive* [9], [23], [24], [41], [57], [59]. The goal of GPM is to find all embeddings that match specific patterns [2]. The tasks are more challenging since the number of embeddings could be large. For example, with WikiVote, a small graph with merely 7k vertices, the number of vertex-induced 5-chain embeddings can reach 71 billion.

Accelerating the performance of a specific application needs to consider two aspects: *memory efficiency and computation efficiency*. The graph computation is typically expressed in the "think like a vertex" (TLV) model [38] in the graph processing systems [12], [20], [37], [38], [43], [53], [67] and architectures [2], [11], [56], [66], [68]. In the iterative graph computation, while the computation that generates the compute array updates is typically lightweight, these updates incur random accesses. Thus, the main challenge is the inefficient memory access due to poor locality and high memory bandwidth consumption. The accelerators mainly focus on hiding communication latency [68], reducing data movements with Processing-In-Memory (PIM) architecture [11], [56], [66], [68], and acceleration of asynchronous [44], [62], [63] and iterative [46] graph processing. Before discussing the architectural implications of GPM, let us consider the two major GPM methods.

The first method is *exhaustive check*: the algorithm enumerates all subgraphs with size up to the pattern size—regardless of the specific patterns. During the subgraph expansion process, some infeasible combinations that cannot match the whole pattern can be pruned early. When the subgraphs reach the pattern size, isomorphic [3] check is performed between each candidate and the pattern graph, if passed, a valid embedding is identified. It is used in the early graph mining system Arabesque [57]. The second method is *pattern enumeration*, which specifically generates the embeddings that satisfy the pattern *by construction*. It avoids the expensive isomorphic check and does not generate infeasible subgraphs. This method is adopted by recent systems, e.g., AutoMine [41], GraphZero [40], GraphPi [52] and Peregrine [24], which achieved significant speedups over Arabesque. RStream [59] is a single-machine system that allows users to express patterns using relational algebra, so that the runtime engine can perform efficient tuple streaming. It lies in between the two method: the join operation does not precisely construct patterns and isomorphic checking is still needed, however; not all subgraphs of the pattern size are enumerated.

---

[1]The codes of [41] are not open source, we implemented InHouseAutomine based on their paper with other optimizations and achieved comparable performance.

[2]While the term "graph mining" is used in some papers such as PEGASUS [25], the system in fact performs typical graph computation, such as computing the diameter of the graph, the radius of each node and finding the connected components. They are not our focus and not accelerated by IntersectX.

[3]Two graphs $G_0 = (V_0, E_0)$ and $G_1 = (V_1, E_1)$ are isomorphic iff. there exists and one-to-one mapping $f : V_0 \to V_1$ such that $(u, v) \in E_0 \iff (f(u), f(v)) \in E_1$.

For GPM, the essential memory access pattern is *edge list access*. For exhaustive check, they are incurred in subgraph expansion [64]. The main source of intensive computation is the expensive isomorphic check. For pattern enumeration, the key operation is the *intersection between two edge lists*, which can construct embedings based on the pattern. For example, for two connected vertices v_1 and v_2, performing the intersection of the two edge lists will identify the triangles (v_1, v_2, v), where v is the neighbor of both v_1 and v_2. During the execution of pattern enumeration, the edge list accesses (memory) and the intersection of edge lists (compute) are performed alternatively.

This paper focuses on pattern enumeration since is significantly faster than exhaustive check. The first graph mining accelerator GRAMER [64] provides the architectural supports for exhaustive check. In Section II-C, we show that the pattern enumeration on an unmodified CPU is likely to run faster than the accelerated exhaustive check with GRAMER. It shows the importance of developing a specialized architecture for the state-of-the-art method. For pattern enumeration, *we focus on the computation efficiency (intersection) rather than memory efficiency for two reasons*. First, the edge list access incurs just *two random accesses*: one to get the pointer to the start of the list and the other to access it. This is much less than the vertex updates in the iterative graph computation—*one random access for each edge*. The majority of accesses—the traversal of all neighbors in the list—are sequential.

Second, we show that the conventional processor cannot execute the intersection efficiently (Section II-B). Thus, *the more expensive computation becomes the bottleneck for GPM*. The current architectures that optimize intersection are either designed for tensor computations [19], [21], or are infeasible to execute the complex code patterns [10], [60] in GPM, such as computation reuse and symmetric breaking [40], [41], [52], without significant efforts. Section II-C will discuss the state-of-the-art GPM algorithm and optimizations.

With the understanding of the architectural challenges and requirements of pattern enumeration based GPM, this paper proposes *IntersectX*, a *vertically* designed accelerator based on *conventional* processor to accelerate GPM by making streams first-class citizens in the ISA. We define a sparse vector as a *stream*, which can be a *key* or *(key,value)* stream. Our novel stream ISA extension *intrinsically operates on streams*, realizing both data movement and computation. It can be considered as a natural extension to the traditional instructions for ordinary scalar values. The IntersectX architecture is composed of specialized mechanisms that efficiently implement the stream ISA extensions, including: (1) Stream Mapping Table (SMT) that records the mapping between the stream ID and the stream register; (2) the read-only Stream Cache (S-Cache) that enables efficient stream data movements; (3) tracking the dependency between streams with a property of intersection; (4) Stream Value Processing Unit (SVPU) that implements sparse value computations; and (5) the nested intersection translator that generates micro-op sequences for implementing nested intersections.

To provide good programmability, similar to Automine [41], we also provide a GPM compiler to generate stream ISA based GPM implementation. Thus, users do not need to write any assembly codes. Our compiler takes one or multiple patterns as input, synthesizes the pattern enumeration algorithms with the intersection related operations, and generates C++ implementations embedded with stream ISA assembly instructions. The main challenge for code generation is stream management (similar to register allocation in traditional compilers). Section V-C will discuss our solution in detail.

Applicability The IntersectX ISA is *flexible*—sufficient to support advanced optimizations used in the leading GPM systems such as Automine [41], Peregrine [24], and GraphPi [52]. We discuss these optimizations in Figure 2 and show how IntersectX implements them in Figure 4. Our ISA is also *general*: it not only accelerates pattern enumeration but also the general tensor computation on sparse data. It cannot benefit Pangolin [9], which is based on exhaustive check but the novel low-level APIs allow efficient filtering of infeasible subgraphs and many optimizations. However, the users of Pangolin is expected to write GPM algorithms and optimizations using the APIs, thus the system is much more difficult to use. We strongly believe the compiler-based approach has major advantage by hiding all implementations details from the users. Moreover, it has been shown that pattern enumeration method can also run faster than Pangolin on CPU (Table 5 of [8]). Finally, we emphaize that the code patterns of pattern enumeration are not suited for GPU. In Section VI-E, we compare the performance of IntersectX with several manually implemented algorithms in GPU.

We implement IntersectX ISA and its architectural components on zSim [50]. We use seven popular GPM applications (triangle/three-chain/tailed-traingle counting, 3-motif mining, 4/5-clique counting, and FSM) on ten real graphs. The results show that IntersectX significantly outperforms the InHouse-Automine on CPU, on average $10.7\times$ and up to $83.9\times$; and GRAMER, a state-of-the-art graph mining accelerator, based on exhaustive check, on average $40.1\times$ and up to $181.8\times$.

II. BACKGROUND

A. GPM Methods and Optimizations

A graph G is represented by its vertex set V and edge set E. GPM applications take an input graph and a pattern graph as inputs, enumerate all subgraphs matching a user-provided pattern, and extract useful information from them. The subgraphs isomorphic to the pattern are named *embeddings*.
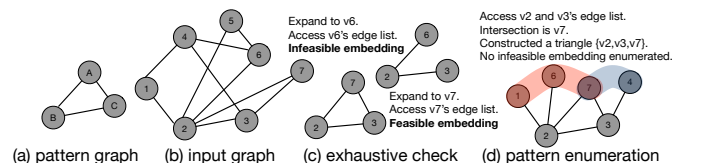

Fig. 1: Graph mining and two methods

Figure 1 shows the GPM problem which finds the pattern (triangle) (a) in the input graph (b). Figure 1 (c) highlights the

subgraph expansion in exhaustive check. Suppose the current subgraph size is 2, they are expanded into size-3 subgraph from one of the vertices. Then the new vertex's edge list is accessed to construct size-3 subgraphs, some of them are infeasible and can be filtered with user-defined filter function. It leads to excessive edge list accesses. Figure 1 (d) shows the memory access and computation of pattern enumeration. From two connected vertices, their edge lists are accessed, followed by the *intersection* between them. In this example, each common neighbor forms a triangle embedding matching the pattern. While edge list accesses are still required, they are followed by the computation (intersection) that is much more complex than graph computation and cannot be efficiently performed in current processors. Moreover, since no infeasible subgraphs are enumerated, the total number of edge list accesses is also less.
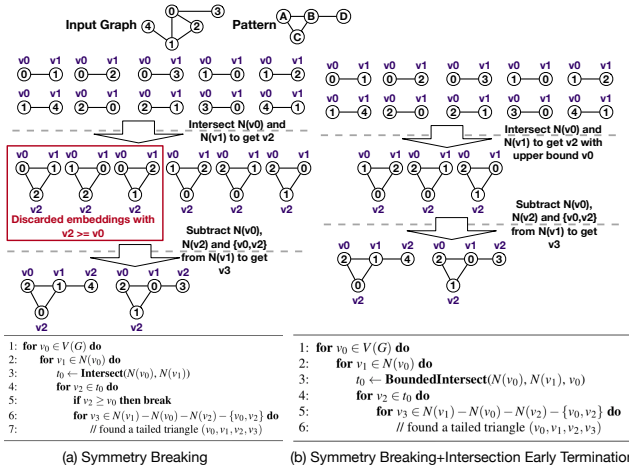

Fig. 2: Tailed-triangle mining

Symmetry breaking in pattern enumeration avoids counting the same embedding for multiple times due to symmetry by enforcing a set of restrictions among vertices during embedding construction. A tailed-triangle mining example is shown in Figure 2. We denote the first/second/third/forth matched vertex of an embedding as v_0-v_3. Symmetry breaking requires $v_2 < v_0$ so that the a unique embedding is enumerated only once, i.e., $(v_0, v_1, v_2, v_3) = (2, 1, 0, 4)$ is the same as $(0, 1, 2, 4)$. As shown in (a), symmetry breaking first obtains all v_2 that is a common neighbor of v_0 and v_1 by intersecting $N(v_0)$ and $N(v_1)$, where $N(v)$ is the neighbor vertex set of v. Then, it discards all v_2 that are no less than v_0 to satisfy the restriction (line 5-6 of the algorithm (a)). This can be improved by *early termination* of intersections since only the elements smaller than v_0 in $N(v_0) \cap N(v_1)$ are needed, indicated as `BoundedIntersect()` in (b). This optimization not only reduces the computation and accessed data in the edge list, but also eliminate branches in the next loop level.
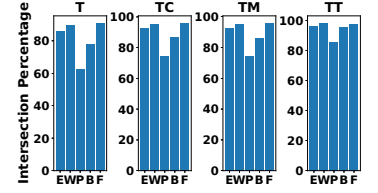
B. Architecture Challenges

Figure 3 shows the example code that performs intersection operation. We abstract the edge lists as `stream1` and `stream2`. If the end of streams have not been reached, the

(a) Intersection Pseudocode

(b) Intersection Percentage in Total Runtime

Fig. 3: Intersection operations

processor reads from `stream1` and `stream2`, and compare the values. If they match, the processor advances the output pointer, writes back to the output array, advances pointers of `stream1` and `stream2`, and checks for boundary for both pointers. If the values mismatch, the processor advances the pointer of one of the streams, checks the boundary, fetches stream data, and compares again. This code pattern contains branches and data dependencies in a tight loop, making it difficult to predict the branches and exploit instruction level parallelism. Figure 3 shows the percentage of cycles in a real machine for executing intersection operations for mining four patterns—Triangle(T), Three chain(TC), Three motif(TM), and Tailed triangle(TT)—on five data sets: patent(P), soc-sign-bitcoinalpha(B), email-eu-core(E), socfb-Haverford76(F), and wiki-vote(W). We see that intersection operations constitute major percentages of execution time. These results justify our focus on improving the computation efficiency of GPM algorithms.

C. Can Existing Architectures Help?

The support for intersection has been proposed in the recent accelerator architectures for DNNs and sparse tensors because it is a key primitive to identify the effectual computations, e.g., the multiplication of *two non-zeros*. Specifically, Extensor [21] uses intersection as the building block to construct sparse tensor algebra kernels, and develops a general architecture to efficiently speed up tensor operation. SparTen [19] is a more specific sparsity-aware DNN accelerator that performs dot-products of two vectors using intersection. The two architectures differ in (1) how the intersection operation is implemented: content addressable memory (CAM) based scan and search in Extensor versus prefix-sum in SparTen; and (2) the generality: an architecture for the general sparse tensor computation (Extensor) or specifically targeting DNN acceleration (Sparten). On the other side, Sparse Processing Unit (SPU) [10], [60] proposes specialized supports for stream-join (similar to intersection) based on a systolic decomposable granularity reconfigurable architecture (DGRA). It uses pipeline to hide the latency of stream-join with a novel design of dataflow control model [10].

However, none of the three architectures can efficiently support pattern enumeration. First, the algorithm cannot be easily expressed in matrix operations. The matrix-based GPM algorithm is either for simple pattern [39] or for specific pattern [18], and are not used in the state-of-the-art general-purpose GPM systems. For this reason, it is almost impossible to port pattern enumeration algorithm to Extensor or SparTen

which are specialized for tensor kernels and BLAS routines. Second, pattern enumeration relies on various optimizations to achieve good performance, including computation reuse, symmetry breaking, and early intersection termination [24], [40], [41], [52]. As shown in Figure 2, they lead to complex code patterns that are infeasible to execute efficiently without significant efforts on the more "general" specialized architectures such as SPU [10], [60]. Specifically, SPU requires manually rewriting C codes and describing data flow graph (DFG) with the language extensions for DGRA. The computations are mapped to the systolic DGRA by analyzing the DFGs. The complexity of pattern enumeration algorithms leads to large DFGs, making it extremely difficult to port to SPU.

GRAMER [64] is the first GPM architecture. However, it is designed for the much slower exhaustive-check method. The key idea is using a heuristic algorithm to classify graph data into high and low priority by approximately simulating the vertex and edge accesses during exhaustive-check in a preprocessing step. Then the high-priority data are permanently stored in the fast memory while the low-priority data are organized in the cache with a specialized data replacement policy. GRAMER achieves impressive speedups compared to two recent GPM frameworks on CPU—$1.11\times \sim 129.95\times$ over RStream [59] and Fractal [14]. Due to the large performance gap, GRAMER running exhaustive check method is very likely to be slower than pattern enumeration on unmodified CPU. Even for small patterns like triangle counting, Automine can be $68.6\times$ faster than RStream; for more complex patterns, it can achieve $777\times$ speedup. This comparison reveals the importance of the superior algorithm, and it is critical to develop architectural supports based on the state-of-the-art method.

D. Design Principle

Our design principle is to develop architectural supports based on the conventional processor, instead of designing an accelerator for graph mining from the ground up. It is justified by the complex control flows and code patterns of the state-of-the-art pattern enumeration algorithms with advanced optimizations. In the next two sections, we will describe our novel *vertical approach, IntersectX*, from the instruction set extension for streams (Section III) to the architecture components that implement the new instructions (Section IV).

III. STREAM ISA

For GPM, the key operation is the intersection between two sparse vectors, e.g., edge lists. In general, we define a sparse vector as a *stream*, which can be: (1) a *key stream*— a list of *keys*, such as the edge list in graph representation; or (2) a *(key,value) stream*—a list of *(key,value)*, such as the pair of indices of non-zero elements and their values in a sparse matrix representation. We propose a novel instruction set extension that *intrinsically operates on streams*, supporting both data movement and computation. The proposed stream ISA extension can be considered as a natural extension to the traditional instructions for ordinary scalar values.

A. Register Extension

The stream ISA extension represents stream as the first-class data type. The processor uses N *stream registers* to maintain stream information, where N is the maximum number of active streams supported. A stream is *active* between its initialization and free—each can be performed by an instruction. A stream register stores the stream ID, the stream length, the start key address, the start value address, and a valid bit. The stream registers cannot be accessed by any instruction and is setup up when the corresponding stream is initialized. The program can refer to a stream by the stream ID, the mapping between a stream ID and its stream register is managed internally in the processor with the *Stream Mapping Table (SMT)* (see details in Section IV-B). The key and value address of a stream register are only used by the processor to refer to the keys and values when the corresponding stream ID is referenced.

We also add three registers to keep the information about compressed sparse row (CSR) graph format [6]. They hold pointers to CSR index, CSR edge list, and CSR offset and can be initialized by an instruction. The CSR offset stores the offset of the the smallest element larger than the vertex itself in the neighbor list. It is used to support the nested intersection, and the symmetric breaking optimization. The design can be adapted to other sparse representations.

B. Instruction Set Specification

Table I lists the instruction set extension for streams. The instructions can be classified into three categories: (1) stream initialization and free; (2) stream computation; and (3) stream element access. The input operands for all instructions are general purpose registers containing stream ID. There is no reason immediate values cannot be used directly as the inputs—we just assume the register operands for simplicity, the same architecture can support both scenarios.

`S_READ` and `S_VREAD` are the instructions to *initialize* a key stream and (key,value) stream, respectively. The operands are general purpose registers containing start key address (also start value address for `S_VREAD`), stream length, and stream ID. After they are executed, if the stream ID is not active, an unused stream register (valid bit is 0) will be allocated to the stream and the new mapping entry is created and inserted into SMT. If the stream ID is already active, the previous mapping is overwritten with the current stream information. After creating the mapping to a stream register, both instruction will also trigger the fetching of *key stream* to the stream cache (see details in Section IV-C). Thus, if the current stream overwrites the previous one, the content in the stream cache will also be updated. Note that `S_VREAD` does not load the values, which will be triggered when the computation instruction for (key,value) stream (`V_VINTER`) is executed. The values are accessed and fetched through the ordinary memory hierarchy rather than the stream cache. `S_FREE` is used to free a stream. When it is executed, the processor finds the SMT entry for the stream ID indicated in the operand and set the valid bit to 0. If such entry is not found, an exception is raised.

Instruction	Description	Operands
S_READ R0, R1, R2	Initialize a key stream	R0:start key address, R1:stream length, R2:stream ID
S_VREAD R0, R1, R2, R3	Initialize a (key,value) stream	R0:start key address, R1:stream length, R2:stream ID, R3:start value address
S_FREE R0	De-allocate a stream	R0:stream ID
S_FETCH R0, R1, R2	Return one element of a key stream	R0:stream ID, R1:element offset, R2: returned element
S_SUB R0, R1, R2, R3	Subtraction of two streams, use stream of id R0 to subtract stream of id R1	R0,R1: input stream IDs, R2:output stream ID, R3: upper-bound of the subtracted result
S_SUB.C R0, R1, R2, R3	Return # of elements in subtraction of two streams, use stream of id R0 to subtract stream of id R1	R0,R1: input stream IDs, R2:returned result, R3: upper-bound of the subtracted result
S_INTER R0, R1, R2, R3	Intersection of two streams	R0,R1: input stream IDs, R2:output stream ID, R3: upper-bound of the intersected result
S_INTER.C R0, R1, R2, R3	Return # of elements in intersection of two streams	R0,R1: input stream IDs, R2: returned result, R3: upper-bound of the intersected result
S_VINTER R0, R1, R2, IMM	Sparse computation using the values of two (key,value) streams	R0,R1: input stream IDs, R2:returned result, IMM: specify user-defined op
S_CSR R0, R1, R2	Register pointers to CSR graph structure	R0:CSR index address, R1:CSR edge list, R2:CSR offset
S_NESTINTER R0, R1	Nested intersection	R0: stream ID, R1: returned result

TABLE I: Stream ISA Extension. R0-R3 are general-purpose registers, IMM is an immediate value.

Our ISA extension contains six instructions for *stream computation*. S_INTER, S_INTER.C, S_SUB, S_SUB.C perform the simple computation on key stream—intersection and subtraction. The suffix ".C" indicates the variants of the corresponding instructions that do not output the result stream but just the *count* of non-zeros in the result stream. If the output is a stream, the stream ID of an initialized stream should be given in one of the input registers. The stream ID will then be added into SMT.

All these instructions take a upper-bound operand R3 to support early intersection/subtraction termination. Once all output stream elements smaller than R3 have been produced, the instruction terminates the computation early. For unbounded operations, R3 is set to −1. It is used to implement the early terminate optimization shown in Figure 2 (b). The conditional termination can be easily implemented inside the intersection unit. Next, we explain the two complex instructions.

The first one is S_VINTER, which performs the user-defined intersected value computations. The instruction first computes the *intersection of the keys* of the two input (key,value) streams, and then performs the *computation on the values* corresponding keys. For example, the key intersection of two (key,value) streams $[(1, 45), (3, 21), (7, 13)]$ and $[(2, 14), (5, 36), (7, 2)]$ is 7. The instruction performs the computation on the corresponding values: assuming the computation is multiply-accumulation (MAC) specified in IMM, the result is $13 \times 2 = 26$ in R2. The other types of computation can be specified in IMM, such as MAX (choose the maximum and accumulate), MIN (choose the minimum and accumulate), or any reduction operation. In IntersectX architecture, the computation on values is performed by a dedicated functional unit, which can be easily extended to perform new operations. This instruction is useful in sparse matrix computation, where the keys indicate the positions of the non-zeros and the actual computations are performed on these values. It is not used in GPM since there is no value involved. If any input stream ID is not a (key,value) stream, an exception is raised.

The second complex instruction is S_NESTINTER, which performs the *nested intersection*. It is an instruction specialized for GPM. Let the input stream (an edge list) be $S = [s_0, s_1, ..., s_k]$, where each s_i corresponds to a vertex. Let us denote the edge list of each s_i as $S(s_i)$, and the result of the instruction as C. This instruction performs the following computation: $C = \sum_{i=0}^{i=k} count((S \cap S(s_i)))$, where $\cap$ is the intersection between two key streams, and *count* returns the length of a stream. The intersections are bounded by the value of s_i. Thus, this instruction implements a kind of *dependent*

```
for (Vertex v0: graph) {
  Set n0 = v0.neighbors();
  // equivalent to
  // cnt+=NestedIntersect(n0)
  for (Vertex v1: n0) {
    Set n1 = v1.neighbors();
    cnt += Intersect(n0,n1).size();
  }
}

... // for (v0: graph)
// R1-R3: start_addr, len, id of n0
S_READ R1,R2,R3
S_NESTINTER R3, R4
S_FREE R3
ADD R5, R4, R5//cnt+=NestedIntersect(n0)
```

(a) Nested Intersection (triangle)

```
for (Vertex v0: graph) {
  Set n0 = v0.neighbors();
  for (Vertex v1: n0) {
    Set n1 = v1.neighbors();
    Set t0 = BoundedIntersect(n0,n1,v0);
    for (Vertex v2: t0) {
      ... // calculate N(v1)-N(v0)
      // -N(v2)-{v0,v2}
    }
  }
}

... // for (v0: graph) for (v1: n0)
// R1-R3: start_addr, len, id of n0
// R4-R6: start_addr, len, id of n1
// R7: id of t0, R8: v0
S_READ R1, R2, R3 // create the input streams
S_READ R4, R5, R6
S_INTER R3, R6, R7, R8 // R8=v0 is the upperbound
S_FREE R3; S_FREE R6 // free the input streams
... // for (v2: t0) ...
```

(b) Bounded Intersection (tailed-triangle)

Fig. 4: Pattern enumeration with Stream ISA Extension

stream intersection. Given a stream S, the other streams to be intersected with it are determined by the keys (vertices) of S. The generation of the dependent streams corresponding to each s_i is performed by the processor using the information in the three CSR registers, which are loaded once using S_CSR before processing a graph.

The S_FETCH instruction performs the *stream element access*—returning the element with a specific offset in a stream, which can be either the output stream of an intersection operation or an initialized stream loaded from memory. Typically, the offset is incremented to traverse all elements in a stream. When it reaches the end of the stream, S_FETCH will return a special "End Of Stream (EOS)" value.

C. Code Examples

Figure 4 (a) shows how to implement triangle counting using our ISA extension. The v1 for-loop is essentially a nested intersection operation on n0. Thus, we can nicely use S_NESTINTER to implement it. There is only one active stream whose ID is stored in R3. The multiple intersections performed by S_NESTINTER do not take stream register resource. In addition, there is only one level of loop in the assemble code. Such specialization based on the understanding of the GPM code pattern is critical to achieving high performance. Figure 4 (b) shows the implementation of tailed-triangle mining (shown in Figure 2 (b)) with intersection early termination. The intersection inputs n0 and n1 are loaded into two streams with IDs R3 and R6, respectively. We then use S_INTER to intersect them with an upper-bound v0 (stored in R8) so that the intersection can terminate early.

Note that our ISA allows different loop iterations to use the same stream IDs, similar to the same variable names. The processor internally keeps track of the active streams in both front-end (after instruction decoding) and back-end (at

instruction commit time), and will recognize the same stream IDs in different iterations as different streams.

```
1   while(true){
2     cmp = stream1[i1] - stream2[i2]
3     if(cmp == 0){
4       i1++;i2++;
5       output += value1[i1]*value2[i2];
6     }else if(cmp < 0){
7       i1++;
8     }else{
9       i2++;
10    }
11    if(i1>boundary1 || i2>boundary2)
12      break;
13  }
```

(a) Sparse computation in C

```
1   ...
2   //mov index addr, length, id, value addr of
         vector 1 to R8-R11
3   S_VREAD R8, R9, R10, R11
4   //mov index addr, length, id, value addr of
         vector 2 to R8-R11
5   S_VREAD R8, R9, R10, R11
6   //mov id of vector 1, vector 2 to R8-R9
7   S_VINTER R8, R9, R10, MAC
8   //mov id of vector 1 to R8
9   S_FREE R8
10  //mov id of vector 2 to R8
11  S_FREE R8
12  ...
```

(b) Sparse computation with our ISA

Fig. 5: Sparse vector multiplication with Stream ISA Extension

Figure 5 (a) and (b) show the vector multiplication implementation with our stream ISA extension. At line 3 and 5, two (key,value) streams are initialized using the addresses of two sparse vectors with S_VREAD. Line 7 performs the multiply-accumulation on the values of the intersected keys.

IV. INTERSECTX ARCHITECTURE

A. Overall Architecture

The IntersectX architecture is composed of specialized structures built on conventional processor architecture and memory hierarchy that implement the stream ISA extensions. Figure 6 shows a detailed overview with stream related components highlighted in gray color. All instructions in Table I except S_NESTINTER occupy one entry in the Reorder Buffer (ROB). To support the ISA extension, the architecture needs to solve a number of problems: (1) the mapping between stream ID and stream register, which is handled by the Stream Mapping Table (SMT); (2) the movement of stream data, which is supported efficiently by the stream cache (S-Cache); (3) the dependency between streams, which is tracked with a property of intersection and minor supports in S-Cache; (4) the implementation of S_VINTER, which is realized by the coordination among the Intersection Unit (IU), Stream Value Processing Unit (SVPU), and the load queue

Fig. 6: IntersectX Architecture

augmented with stream information; (5) the implementation of S_NESTINTER, which is realized by the nested intersection translator that generates the micro-op sequence, similar to the contemporary implementation of CISC instructions with RISC-style micro-ops.

B. Stream ID Mapping

In IntersectX, each stream ID (*Sid*) specified in an instruction is mapped to an internal stream register (*Sreg*). This mapping is performed at the front-end after instruction decoding and the mapping relation is kept in SMT. Besides the stream ID and its mapped stream register, each SMT entry contains: (1) two valid bits: V_D, indicating the *define* point of the stream, and V_A, indicating whether the stream is *active*; (2) the *start (s)* and *produced (p)* bit, which indicate whether S-Cache contains the keys from the start of the stream and whether the data for the whole stream is produced (so that it can be used by the dependent streams); and (3) the *pred0* and *pred1*: the IDs of the streams that the current stream depends on. In this section, we explain the two valid bits and the others will be discussed together with S-Cache and dependence handling.

Initially, both V_D and V_A are 0 and SMT is empty. Both V_D and V_A are set after decoding a S_READ or a S_VREAD instruction and the SMT entry indicates that the Sid_i in the last operand of the instruction is mapped to Sreg_j. Both V_D and V_A are set to one, they indicate that the instruction defines Sid_i and it is active. Later, when S_FREE Sid_i is decoded, the SMT is examined and an entry for Sid_i should be found (otherwise an exception is raised), and its V_D is reset, while V_A is unchanged. This means that Sid_i is no longer defined—the instructions after S_FREE Sid_i should not be able to reference Sid_i—but the stream is still active since S_FREE Sid_i has not been retired. When S_FREE Sid_i is retired, V_A is reset and the entry becomes free. When a new stream is mapped, the processor checks SMT and finds an entry with $V_A = 0$, which implies $V_D = 0$. Note that is not true vise versa—$V_D = 0$ does not imply $V_A = 0$.

Our design expects the codes to call S_FREE after a stream is no longer used, so that its SMT entry can be released. In Section V-B we will describe the APIs for programmers, who do not need to directly write assembly codes, thus this requirement can be easily achieved. When all stream registers are occupied ($V_A = 1$), the instruction that initializes a new stream will be stalled. The larger (or even unlimited) number of stream IDs can be supported by virtualization—by saving some SMT entry to a special memory region to release SMT space. Due to the space limit, we do not discuss this in detail. In fact, using 16 stream registers is enough for all our applications. The design can naturally support the stream operations in loop iterations. Typically, inside an iteration, some streams are initialized and computations on them are performed before S_FREEs at the end of the iteration (refer to Figure 4 (c) for an example). The different iterations can use the same stream IDs, which will be mapped to different SMT entries with our SMT mechanisms.
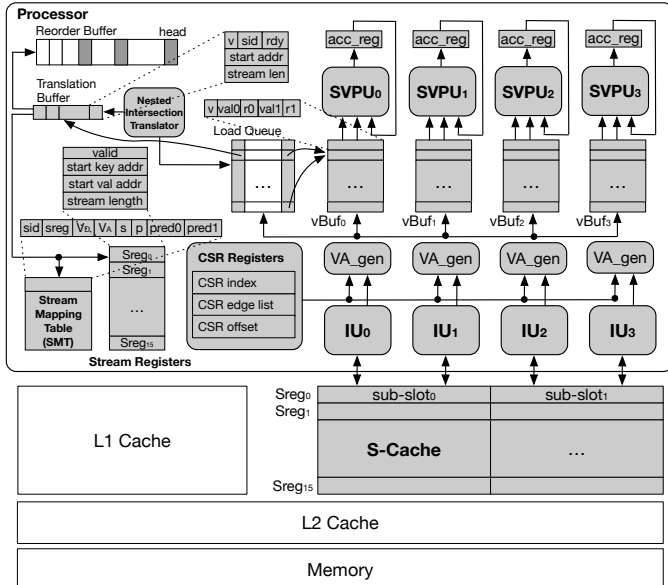
Note that the SMT mechanisms will not increase the latency of CPU pipeline, and they can be implemented in a pipelined manner similar to the register rename stage in CPU. Specifically, the mapping from architecture registers to physical registers is similar to the mapping from *Sids* to *Sregs*. We also maintain the "readiness" of stream IDs.

C. Stream Cache

In IntersectX, the keys for each active stream are loaded into a special *stream cache (S-Cache)*, which is on top of L2 cache together with L1. Note that the values in (key,value) stream are still fetched through the normal memory hierarchy. Thus, when the stream keys are accessed using the stream instructions, the data will not pollute L1. Such specialization enables efficient stream data movements while avoiding cache evictions by other data. Since the keys of a stream are accessed sequentially, the data can be effectively prefetched to S-Cache without a complex prefetcher, thanks to the *known* access pattern. The organization of S-Cache is simple: each stream register has a *slot* that holds a fixed number keys of the stream. We use the 64-key slot which leads to 256 byte slot size. With 16 stream registers, the total size of S-Cache is 4KB.

When an S_READ is executed, the first 64 keys are fetched to the S-Cache, and the *start* bit in SMT for the stream is set. Unless the length of the stream is no more than 64, at this point the S-Cache only contains the first portion of the stream. The *start* bit indicates that the instructions that depend on the stream can use the data in the S-Cache slot. Referring to Table I, our ISA does not contain any instruction that explicitly stores to a stream: only S_INTER and S_SUB produce the results in the destination stream. When these instructions are executed, the result keys are written to the S-Cache slot in group of 64. If the result stream contains more than 64 keys, the slot will contain *the most recently produced 64 keys* while the previous slot is written back to L2 and the *start* bit is cleared. When the whole result stream is generated by the computation instruction, the *produced* bit is set, which is used to trigger the dependent instructions.

The typical code pattern is that two streams are initialized by S_READ before the intersection operation is performed. In this case, data fetching from L2 to S-Cache and transfer to IUs for computation can be pipelined. To support that, we use the idea of double buffer and divide each slot into two sub-slots. When a sub-slot is fetched from L2, the keys in the other sub-slot can be prefetched to IU simultaneously and the intersection computation can be overlapped. We assume that the bandwidth between the stream cache and IU is 4 keys (16 bytes) per cycle, which is similar to the read bandwidth of L1 cache of Intel Nehalem at 128 bits per cycle [22].

Typically, the intersection computation time of a sub-slot (e.g., 32 to 64 cycles) is longer than fetching data from L2 on cache hits (e.g., 20 cycles). With multiple IUs, the parallel execution time of multiple intersections can be better overlapped with the data fetching time of these streams. When multiple IUs (4 in our design) need data to perform computations, S-Cache has to schedule the data transfer to different IUs. We use a simple round-robin policy: at each cycle, S-Cache schedules the transfer of 4 keys to a different IU that is waiting for the data. Each IU is able to perform the intersection on the partial key streams received.

D. Stream Data Dependency

Two streams may have dependency due to: (1) stream ID, where an instruction uses the output stream of a previous computation (S_INTER or S_SUB) as an input stream; or (2) the overlapped memory regions of two streams. It is easy to handle the first scenario: after the stream IDs are available after decoding, the dependency can be handled in the similar manner to the data dependency on general registers. When a dependency is identified, the consumer instruction can only execute after the producer instruction. It is enforced by filling the *pred0* and *pred1* in SMT of the consumer instruction. When the producer instruction finishes, its SMT entry's *produced* bit is set. Each cycle the processor checks the status of the producer instruction(s) and triggers the consumer instruction when all operands' *produced* bit are set. If the key stream produced is less than 64 keys, the whole stream is in S-Cache with the *start* bit set, the consumer instruction reads directly from S-Cache; otherwise, the slot will be refilled from L2.

For the second scenario, we can check the potential dependency conservatively by leveraging the fact that *the length of the output stream is less than the minimum length of the two input streams*. Thus, we can conservatively deduct the maximum length of the output stream. The possibly overlapped stream memory regions can be detected using the start key address and stream length of different streams. The dependent stream instructions need to be executed sequentially, which is enforced using the same mechanism as the first scenario.

E. Sparse Computation on Values

The sparse computation on values is suppored by the coordination between IU, value buffer (vBuf), load queue, and Stream Value Processing Unit (SVPU). When S_VINTER is executed, an IU starts with key intersection calculation and the output keys are given to the *Value Address Generator (VA_gen)* associated with the IU (refer to Figure 6). VA_gen generates the value addresses for each key in the intersection. These addresses are sent to load queue to request the values through the normal memory hierarchy, rather than S-Cache. Each value request is also allocated with an entry in the vBuf, which will collect the two values returned from the load queue (val0 and val1). Each entry has a ready bit (r) for each value, which is set when the load queue receives the value. We assume that the operation is commutative (e.g., multiply-accumulate) thus the computation using val0 and val1 can be performed by SVPU as soon as both ready bits are set. We do not need to enforce any order on the accumulation. The *acc_reg* is used to keep the accumulated partial results. While performing substantial amount of computations, this instruction only takes one entry in ROB. After the final result is produced in the acc_reg of the corresponding IU, it will be copied to the destination register,

and then the instruction will retire from the processor when it reaches the head of ROB.

F. Nested Intersection

The `S_NESTINTER` is the most complex instruction and we use the *Nested Instruction Translator* to generate the instruction sequence of other instructions of stream ISA to implement it. Based on the input key stream, the translator first generates the stream information based on each key element. The memory addresses of the streams information are calculated based on the CSR registers, then the memory requests are sent through load queue. For each stream, an entry is allocated in the *translation buffer*, its ready bit (rdy) is set when the stream information is returned at load queue. Similar to the pointer to vBuf entry, each load queue entry also keeps a pointer to the translation buffer entry. For each nested stream, three instructions are generated: `S_READ`, `S_INTER.C`, and `S_FREE`. An addition instruction is generated to accumulate the counts. Each instruction takes an entry in the translation buffer. The start address and stream length fields are only used in `S_READ`. When the stream information is ready, the three instructions are inserted into ROB. The translation is stalled when the translation buffer is full, which can be due to either ROB full or waiting for the stream information. In either case, the space will later be released because eventually the instructions in ROB will retire and the requested data will be refilled. These events do not wait for the translation procedure thus there is no deadlock.

V. IMPLEMENTATION AND SOFTWARE INTERFACE

A. Implementation Considerations

The `S_NESTINTER` is translated into a variable length instruction sequence by the *Nested Instruction Translator* and will take multiple ROB entries. To ensure the precise exception, the processor takes a checkpoint of registers before the instruction. If an exception is raised during the execution of the instruction sequence, the processor rolls back to the checkpoint and raises the exception handler. It is similar to the mechanisms for transactional and atomic block execution [7], [45]. Besides the normal information such as general registers, the checkpoint includes the content of SMT, stream registers and CSR registers. Another assumption in IntersectX architecture is that the stream cache does not participate in the coherence protocol. Thus, the potential modifications of other cores on key elements do not propagate in time to stream cache. However, for the applications that IntersectX is targeted for, the data (such as graph or sparse matrix) are read-only. Therefore, it does not cause any major problem.

In IntersectX, due to the complex code patterns in pattern enumeration, we *tightly couple* the accelerator units with the processor, rather than building a stand-alone accelerator. A more decoupled architecture would incur relatively high overhead for the interaction between CPU and the accelerator. Nevertheless, with more significant change of the software and an appropriate way to map each function to architecture, it is

VertexSet RegisterVertexSet (**Vertex*** addr, **Length** len)
void ReleaseVertexSet (**VertexSet** handler)
Length NestCounting (**VertexSet** handler)
Vertex EnumerateVertexSet (**VertexSet** handler, **Length** offset)
void SubtractVertexSet (**VertexSet** A, **VertexSet** B, **VertexSet** C, **VertexId** D)
Length SubtractVertexSetCount (**VertexSet** A, **VertexSet** B, **VertexId** C)
void IntersectVertexSet (**VertexSet** A, **VertexSet** B, **VertexSet** C, **VertexId** D)
Length IntersectVertexSetCount (**VertexSet** A, **VertexSet** B, **VertexId** C)
Vector RegisterVector (**Index*** addr, **Value*** addrV, **Length** len)
void ReleaseVector (**Vector** handler)
Value VectorCompute (**Vector** A, **Vector** B, **Op** type)

TABLE II: IntersectX APIs (Function Prototype)

possible to develop a more decoupled accelerator. We leave that as the future work.

B. Hardware Cost

```
1   for(Vertex v1 : graph){
2     Vertex* addr = &v1.neighbor();
3     Length len = v1.neighbor().size();
4     VertexSet set1 = RegisterVertexSet(addr, len);
5     Length counter = 0;
6     while(counter<len){
7       Vertex v2 = EnumerateVertexSet(set1,counter);
8       Length len2 = v2.neighbor().size();
9       Vertex* addr2 = &v2.neighbor();
10      VertexSet set2 = RegisterVertexSet(addr, len);
11      patternNum += SubtractVertexSetCount(set1,set2);
12    }
13  }
```

Fig. 7: API Example: Three Chain

The Coordinator module from ExTensor [21] and the IU of IntersectX have similar functionality—performing intersection logic, and if anything the Coordinator should be more complex. Thus we substitute IU area with Coordinator area. ExTensor lists the total area of Coordinators to be $2.38mm^2$ using 32nm, and with 129 individual coordinators (128 from PE and 1 in LLB), each coordinator is thus 0.0184mm2. The cost of 4 IU in IntersectX is thus $0.0738mm^2$. Similar to ExTensor, we use CACTI [42] to model area for its SRAM components, and stream registers, stream mapping table, and stream cache. At 32nm and with implementation as scratchpad RAM, stream register file takes $0.0008mm^2$, stream mapping table $0.0010mm^2$, and stream cache $0.0175mm^2$, for a total of $0.0193mm^2$. In total, the most additional area for IntersectX (memory and intersection logic) is around $0.0931mm^2$ at 32nm. Of course, actual integration into the cores would require further routing which will increase this number. However we show that the IntersectX hardware modules do not constitute a significant hardware cost.

C. GPM Compiler and Low-Level APIs

IntersectX provides high-level software interface for the typical users of GPM systems, such as scientists and data analysts, who are not algorithm experts. The key is to provide good programmability. To use the high-level interface, the users just need to specify the patterns and the input graph, and the compiler will generate the binary for mining the given pattern(s). Similar to Automine [41], we developed a GPM compiler to generate stream ISA based GPM implementation generation. The compiler takes the user-specified patterns as input, synthesizes the corresponding intersection based GPM algorithms (e.g., those in Figure 2), and translates them to

Number of cores	8
ROB size	128
loadQueue size	32
l1d cache size	64KB
cache line size	64B
l2(last level) cache size	2MB
stream cache latency	1 cycle
stream cache bandwidth	16B
stream cache slot size	256B
l1d latency	4 cycles
l2(last level) cache latency	10 cycles
memory controllers number	3
memory controller latency	40 cycles
memory type	DDR3-1333-CL10

TABLE III: IntersectX Architecture Configuration

C++ implementations embedded with stream ISA assembly instructions.

One major challenge is stream management during code generation (similar to register allocation in traditional compilers). To implement an intersection, the compiler may generate instructions that introduce up to three active streams—two input streams loaded by `S_READ` and one output stream produced by `S_INTER`. We release these created streams eagerly, since resources used to maintain actives streams (e.g. s-cache and stream registers) are limited. The streams created by `S_READ` are released by `S_FREE` after the intersection operation, and the compiler will insert `S_FREE` instructions to free the stream produced by `S_INTER` once it is no longer needed. If the number of actives streams reaches its limit (i.e., the number of stream registers), the compiler simply falls back to generate scalar ISA based intersection code, and print outs a warning message. In practice, we notice that such a "fallback" scenario is rare (and actually did not happen for all applications evaluated in this paper) thanks to our aggressive stream freeing strategy.

IntersectX also provides the low-level programming interface for the experienced users to construct more complex applications such as frequent subgraph mining (FSM). Table II lists IntersectX APIs for building GPM applications by users. Each function can be implemented with the proposed stream ISA extension. Figure 7 shows an example of three-chain algorithm based on the APIs.

VI. EVALUATION

A. Simulator and Configuration

We simulate IntersectX on zSim [50], a fast and scalable simulator designed for x86-64 multicores. We integrate all our proposed architectural components including Stream Cache and Intersection Unit into the simulator. Our configuration is listed in Table III.

B. Graph Mining Algorithms and Data Sets

We execute our InHouse-Automine [41] to mine different patterns. We choose several popular GPM applications listed in Table V

name
Triangle counting (T)
Three chain counting (TC)
Tailed triangle counting (TT)
3-motif (TM)
4-clique (4C)
5-clique (5C)
Frequent subgraph mining (FSM)

TABLE V: Applications

name	#V	#E	avg D	max D
citeseer (C) [4], [17], [49]	3.3K	4.5K	1.39	99
email-eu-core (E) [34], [65]	1.0K	16.1K	25.4	345
soc-sign-bitcoinalpha (B) [1], [28], [29]	3.8K	24K	6.4	511
p2p-Gnutella08 (G) [35], [48]	6k	21k	3.3	97
socfb-Haverford76 (F) [49]	1.4K	60K	41.3	375
wiki-vote (W) [31], [32]	7k	104k	14.6	1065
mico (M) [16]	96.6K	1.1M	11.2	1359
com-youtube (Y) [61]	1.1M	3.0M	2.6	28754
patent (P) [33]	3.8M	16.5M	8.8	793
livejournal (L) [3], [36]	4.8M	42.9M	17.7	20333

TABLE IV: Graph Datasets

to evaluate IntersectX. They can be divided into four categories. (1) *Pattern counting* applications, which include triangle (T), three-chain (TC), and tailed-triangle counting (TT). These three workloads aim to count the number of triangle/three-chain/tailed-triangle embeddings, respectively. We use T, 4C, and 5C to denote the nested implementations while TS, 4CS, and 5CS refer to the corresponding stream implementations without nested support. (2) *k-motif mining*, which counts the embeddings of all connected patterns with a given size k. (3) *k-clique mining*, which discovers all size-k complete subgraphs of the input graph. (4) *Frequent subgraph mining (FSM)*, which aims to discover all vertex-labeled frequent patterns. A pattern is considered as *frequent* if and only if its *support* is no less than a user-specified threshold. Pattern support could have different definitions. However, all of them should satisfy the *Downward Closure Property*, which requires that one pattern should never have a greater support than its subpatterns. This key property is used in FSM to prune the searching space efficiently–if one pattern is infrequent, it can be safely discarded since it cannot be extended to any frequent patterns. Similar to previous systems like Peregrine [24], we choose the *minimum image-based support metric* [5] and only discover frequent patterns with no more than three edges. Besides, it is worth noting that GRAMER *mistakenly* used the pattern count (i.e., the number of embeddings) as the pattern support for FSM, which violates the Downward Closure Property. *We also implement this incorrect FSM algorithm for performance comparison purposes and refer to it as simple-FSM (sFSM) in our experiments*. Table IV lists the real-world graphs we used from various domains, ranging from social network analysis to bioinformatics.

C. Overall Performance

We compare IntersectX with GRAMER [64] and our CPU baseline on different datasets and algorithms.
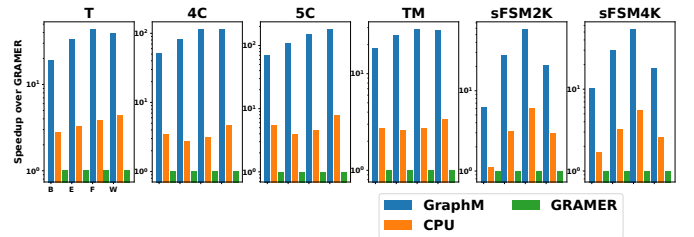

Fig. 8: Speedup of IntersectX and CPU (pattern enumeration) over GRAMER (exhaustive check) (log scale)

1) Comparison with GRAMER: We also implemented GRAMER on zsim. To simplify the comparison, we only enable one PU/CPU core in both GRAMER and IntersectX. In order to make a fair comparison, we configure GRAMER's on-chip RAM access latency to be the same as IntersectX's first level cache latency.

We compare the performance of IntersectX, the CPU baseline, and GRAMER in Figure 8. The applications involved are Triangle Counting, 4/5-Clique, 3-motif, and sFSM with 2K/4K support thresholds. IntersectX significantly outperforms both the CPU baseline and GRAMER. It is worth noting that GRAMER is even slower than our CPU baseline. The performance gap is majorly attributed to the algorithmic difference. Our CPU baseline implements the pattern enumeration method, which is much faster than the exhaustive check method in GRAMER. The architectural supports in GRAMER cannot benefit the pattern enumeration method.

Another key observation is that IntersectX achieves higher speedups over GRAMER for more complex patterns, such as 4/5-clique counting. On average, IntersectX outperforms GRAMER by $85.5\times$, $121.3\times$ for 4-Clique and 5-Clique counting, respectively. By contrast, for triangle counting, the speedup is only $32\times$. The speedup difference is reasonable. As we have discussed in Section II, one major source of exhaustive check method's inefficiency is their connectivity check operations. A larger pattern incurs more connectivity checks. For instance, to extend a size-k subgraph $(v_0, v_1, ..., v_{k-1})$, the exhaustive check method typically selects an existing vertex $v_i (0 \le i \le k-1)$, and choose one of its neighbor $v_k \in N(v_i)$ to be the new vertex. $k-1$ connectivity checks are needed to determine whether v_k is connected with the existing vertices except for v_i. As a result, to enumerate a larger subgraph, exhaustive check systems/accelerators like GRAMER suffer more from the overhead caused by connectivity checks. This explains IntersectX's higher speedup over GRAMER for the larger pattern since it is based on pattern enumeration and totally avoids connectivity checks.

2) Comparison with CPU: Further performance comparison among IntersectX (with/without nested intersection) and the CPU baseline are shown in Figure 9. TS, 4CS, and 5CS refer to the triangle counting, 4-clique, and 5-clique implementations without nested intersection. On average, enabling nested intersection speeds up these applications by $1.357\times$. It is because with nested intersection instructions, the normal instructions used to explicitly manage the corresponding loops, graph structure accesses, and embedding counting are eliminated. Nested intersection instructions allow more intersections execute on-the-fly simultaneously, thanks to the reduction of normal instructions that would have occupied more ROB entries. Besides, note that IntersectX achieves less speedup for FSM. It is because the support calculation in FSM is costly, and thus the intersection/subtraction operations that our architecture accelerates only take a smaller portion of execution time.

Comparing across different datasets, IntersectX achieves higher speedups on graphs with higher average degree. This could be explained by Amdahl's law. On graphs with higher degrees, the operand lengths of intersection/subtraction operations are generally longer. As a result, these operations are more computation-intensive and take up a larger portion of execution time. Recall that IntersectX only speedups intersection/subtraction operations, and thus achieves higher performance improvement on denser graphs.

D. Execution Time of Intersection Operations

We analyze the execution time percentage for intersection operations in IntersectX. The results are shown in Figure 10. We observe that intersection operations still take up a large portion of execution time even though significant acceleration. This indicates that there are plenty of research opportunities to speedup GPM applications by optimizing intersections.

E. Comparing to GPU

We also compare IntersectX with GPU (Nvidia Tesla K40m). We assume the clock frequency of IntersectX to be 1Ghz. We compare the performance of IntersectX (with symmetry breaking) with two GPU implementations with or without symmetry breaking optimizations. The optimization in general adds more branches, and we want to study, with massive parallelism, whether the redundant enumeration with less branch divergence can overshadow less computation with more branches. Figure 11 shows the results. We can see that: 1) IntersectX outperforms the GPU implementations significantly, thus, even with a more powerful GPU, the results should stay the same; and 2) symmetry breaking is also effective in GPU, and the massive parallelism on more computation cannot overweight less computation with more branches. Using Nvidia profiling tools, we find that the reason for low performance of pattern enumeration on GPU is two-fold: 1) low warp utilization (about 4.4%) due to the branches and the different loop sizes (edge list length) for different threads; and 2) low global memory bandwidth utilization (about 13%) since threads access edge lists at different memory locations. Based on our results, it is no surprise that all existing pattern enumeration based graph mining system are based on CPU.

F. The Distribution of Stream Lengths

We further analyze the length distribution of involved streams in different GPM algorithms. Figure 14 (a) shows the cumulative distribution function (CDF) of stream lengths in different graph mining algorithms on the email-eu-core graph. Even on the same graph dataset, different applications could lead to different stream length distributions. We notice that clique applications (i.e., 4-clique/5-clique counting) in general introduce shorter stream lengths. The reason is that in clique applications, the input operands of intersection operations are usually the intersection results of other streams. And these operands tend to have shorter stream lengths.

We also fix the graph mining application to triangle counting and analyze the stream length distribution on various datasets. The results are reported in Figure 14 (b). For this figure, we cut off the counting for stream larger than 500. The
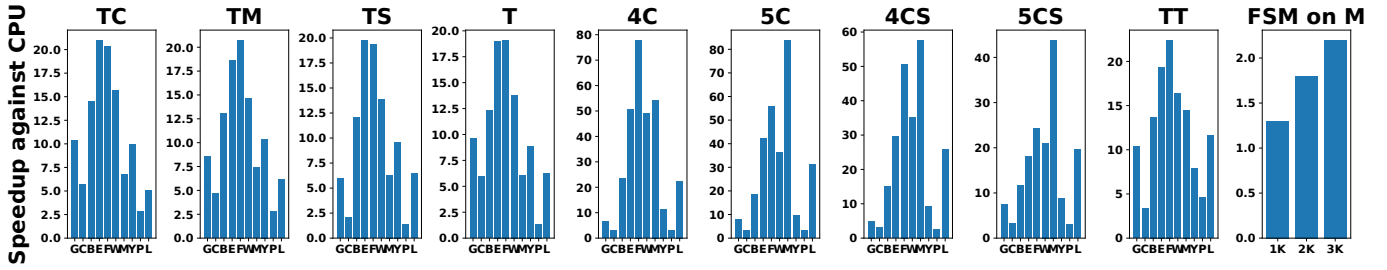
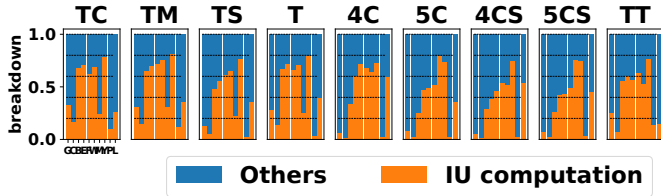Fig. 9: Speedups over CPU (Both use pattern enumeration)

Fig. 10: Execution Time Percentage of Intersections

Name	Dimensions	Nonzeros	Sparsity
Circuit204 (C) [13]	1020×1020	5883	0.57%
Email-Eu-core(E) [34], [65]	1005×1005	25571	2.5%
Fpga_dcop_26 (F) [13]	1220×1220	5892	0.40%
Piston (P) [13]	2025×2025	100015	2.4%
Laser (L) [13]	3002×3002	5000	0.055%
Grid2 (G) [13]	3296×3296	6432	0.059%
Hydr1c (H) [13]	5308×5308	23752	0.084%
California (CA) [27], [30]	9664×9664	16150	0.017%
Chicago Crime (Chi) [54]	$6186 \times 24 \times 2464$	5330673	1.46%
Uber Pickups (U) [54]	$4392 \times 1140 \times 1717$	3309490	0.0385%

TABLE VI: Matrix and tensor Datasets

observation is intuitive–the longest stream length on datasets with larger maximal degrees (e.g., LiveJournal, Youtube) are longer. Besides, there are more long streams on denser datasets like E (email-eu-core) and F (socfb-Haverford76).

G. Varying the Number of Intersection Units

We characterize the performance of IntersectX by varying the number of IUs. Figure 12 shows the results with 1 to 16 intersection units. When the number of IUs is no more than 4, increasing it will generally improve IntersectX's performance. However, with more than 4 intersection units, adding IUs introduces significantly less benefit or even slight performance degeneration. The non-monotonic behavior when increasing the numbers of IUs can be explained as follows. We find that the miss rate in L2 cache is increased in these cases. We believe this is due to the different IUs trying to read streams from different memory addresses, which leads to relatively more random requests to L2. Thus increasing IU number may lead to higher conflict in LLC. This indicates that the different architecture components need to be matched based on performance characterization.

H. Analysis on S-Cache Bandwidth

We further characterize IntersectX's performance with different S-Cache bandwidths. Figure 13 shows the performance of IntersectX with S-Cache bandwidth varying from 2 elements (64 bits) per cycle to 32 elements (1024 bits) per cycle. In general, increasing S-Cache bandwidth can improve IntersectX's performance. However, there is a point of diminishing return. For example, for the TC (three-chain counting) application, increasing the bandwidth from 4 to 32 elements/cycle introduces almost no benefit. It is because there are not enough concurrent active stream intersection/subtraction operations to saturate the S-Cache bandwidth. The number of concurrent active stream operations is determined by the application and implementation. Triangle counting (T) and 4/5-Clique (4/5C) counting use the nested intersection instruction to trigger

intersection operations in a bursty manner, and thus there are more simultaneously on-the-fly intersections. Hence, T/4C/5C benefits more from S-Cache bandwidth increase than other algorithm/implementation without the nested instruction (e.g., 4CS, 5CS). Moreover, each algorithm has a unique intersection pattern, which leads to different number of simultaneously on-the-fly intersections. Therefore, each algorithm would benefit from the S-Cache bandwidth increase differently.

I. Tensor Computation

To evaluate Stream Value Processing Unit (SVPU) of IntersectX, we implemented sparse matrix multiplication, tensor times vector (TTV, $Z_{ij} = \sum_k A_{ijk}B_k$) and tensor times matrix (TTM, $Z_{ijk} = \sum_l A_{ijl}B_{kl}$) with our (key,value) stream interfaces. For sparse matrix multiplication, we convert the matrix format from Compressed Sparse Row (CSR) to Compressed Sparse Column(CSC) and multiply the column of CSR with the row of CSC. For tensor times vector and tensor times matrix, we store the tensor in CSF [55] format and the vector as sparse vector. We use state-of-the-art tensor algebra compilers (TACO [26]) to generate baseline tensor kernel.

We evaluated IntersectX with matrices and tensors listed in Table VI. The speedup of IntersectX against the CPU baseline is shown in Figure 15. For sparse matrix multiplication, IntersectX achieves on average $5.7\times$ speedup. For matrices with higher density, IntersectX can achieve higher speedup. The reason is, since there are more non-zeros, denser matrices lead to more intersection computation, which can be accelerated by IntersectX architecture. For tensor computation, IntersectX achieves on average $6.08\times$ speedup. Similar to matrices, for tensor with higher density, IntersectX can achieve higher speedup.

VII. Conclusion

This paper proposes IntersectX, a vertically designed accelerator for GPM applications with stream instruction set
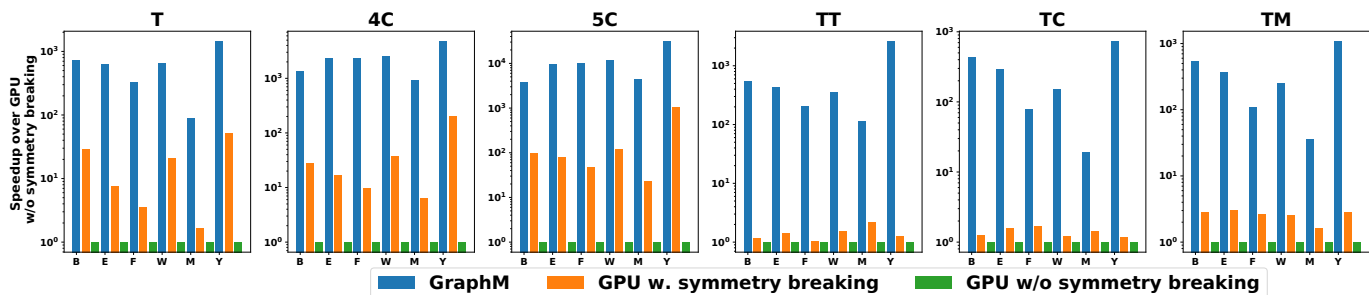
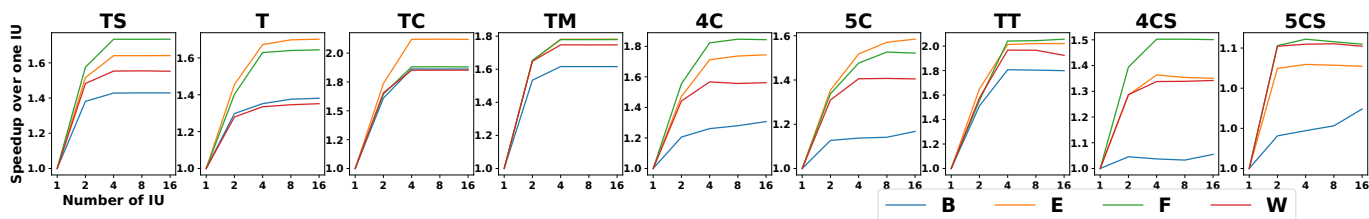Fig. 11: IntersectX compared to GPU implementations (log scale)

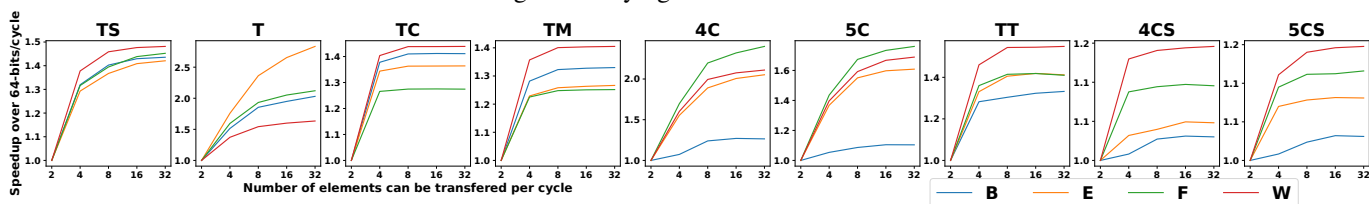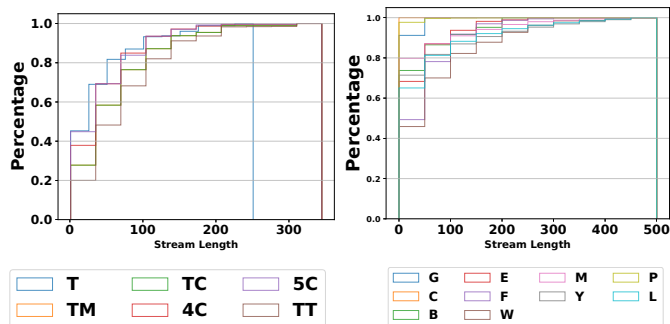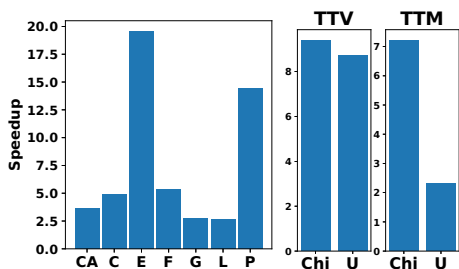Fig. 12: Varying the Number of IUs

Fig. 13: Varying S-Cache Bandwidth

(a) Different Patterns on Email-Eu-Core (b) Triangle Counting on Different Graphs

Fig. 14: The Stream Length Distribution

(a) Sparse Matrix Computation (b) tensor times vector

Fig. 15: (key,value) Stream Computation Speedup

extension and architectural supports based on conventional processor. We develop the IntersectX architecture composed of specialized mechanisms that efficiently implement the stream

ISA extensions. We develop the IntersectX architecture composed of specialized mechanisms that efficiently implement the stream ISA extensions. We implement IntersectX ISA and architecture on zsim [50]. We use 7 popular GPM applications (triangle/three-chain/tailed-traingle counting, 3-motif mining, 4/5-clique counting, and FSM) on 10 real graphs. Our extensive experiments show that IntersectX outperforms our CPU baseline and GRAMER significantly. The average speedups could be up to 83.9×and 181.8×and on average 10.7×and 40.1×, respectively.

REFERENCES

[1] "Bitcoin alpha network dataset – KONECT," Feb. 2018. [Online]. Available: http://konect.cc/networks/soc-sign-bitcoinalpha

[2] J. Ahn, S. Hong, S. Yoo, O. Mutlu, and K. Choi, "A scalable processing-in-memory accelerator for parallel graph processing," in *Proceedings of the 42nd Annual International Symposium on Computer Architecture*, 2015, pp. 105–117.

[3] L. Backstrom, D. Huttenlocher, J. Kleinberg, and X. Lan, "Group formation in large social networks: membership, growth, and evolution," in *Proceedings of the 12th ACM SIGKDD international conference on Knowledge discovery and data mining*, 2006, pp. 44–54.

[4] D. A. Bader, H. Meyerhenke, P. Sanders, and D. Wagner, *Graph partitioning and graph clustering*. American Mathematical Society Providence, RI, 2013, vol. 588.

[5] B. Bringmann and S. Nijssen, "What is frequent in a single graph?" in *Pacific-Asia Conference on Knowledge Discovery and Data Mining*. Springer, 2008, pp. 858–863.

[6] A. Buluç, J. T. Fineman, M. Frigo, J. R. Gilbert, and C. E. Leiserson, "Parallel sparse matrix-vector and matrix-transpose-vector multiplication using compressed sparse blocks," in *Proceedings of the twenty-first annual symposium on Parallelism in algorithms and architectures*, 2009, pp. 233–244.

[7] L. Ceze, J. Tuck, J. Torrellas, and C. Cascaval, "Bulk disambiguation of speculative threads in multiprocessors," *ACM SIGARCH Computer Architecture News*, vol. 34, no. 2, pp. 227–238, 2006.

[8] J. Chen and X. Qian, "Dwarvesgraph: A high-performance graph mining system with pattern decomposition," *arXiv preprint arXiv:2008.09682*, 2020.

[9] X. Chen, R. Dathathri, G. Gill, and K. Pingali, "Pangolin: An efficient and flexible graph pattern mining system on cpu and gpu," *arXiv preprint arXiv:1911.06969*, 2019.

[10] V. Dadu, J. Weng, S. Liu, and T. Nowatzki, "Towards general purpose acceleration by exploiting common data-dependence forms," in *Proceedings of the 52nd Annual IEEE/ACM International Symposium on Microarchitecture*, 2019, pp. 924–939.

[11] G. Dai, T. Huang, Y. Chi, J. Zhao, G. Sun, Y. Liu, Y. Wang, Y. Xie, and H. Yang, "Graphh: A processing-in-memory architecture for large-scale graph processing," *IEEE Transactions on Computer-Aided Design of Integrated Circuits and Systems*, 2018.

[12] R. Dathathri, G. Gill, L. Hoang, H.-V. Dang, A. Brooks, N. Dryden, M. Snir, and K. Pingali, "Gluon: A communication-optimizing substrate for distributed heterogeneous graph analytics," in *Proceedings of the 39th ACM SIGPLAN Conference on Programming Language Design and Implementation*, 2018, pp. 752–768.

[13] T. A. Davis and Y. Hu, "The university of florida sparse matrix collection," *ACM Transactions on Mathematical Software (TOMS)*, vol. 38, no. 1, pp. 1–25, 2011.

[14] V. Dias, C. H. Teixeira, D. Guedes, W. Meira, and S. Parthasarathy, "Fractal: A general-purpose graph pattern mining system," in *Proceedings of the 2019 International Conference on Management of Data*, 2019, pp. 1357–1374.

[15] A. Duma and A. Topirceanu, "A network motif based approach for classifying online social networks," in *2014 IEEE 9th IEEE International Symposium on Applied Computational Intelligence and Informatics (SACI)*. IEEE, 2014, pp. 311–315.

[16] M. Elseidy, E. Abdelhamid, S. Skiadopoulos, and P. Kalnis, "Grami: Frequent subgraph and pattern mining in a single large graph," *Proceedings of the VLDB Endowment*, vol. 7, no. 7, pp. 517–528, 2014.

[17] R. Geisberger, P. Sanders, and D. Schultes, "Better approximation of betweenness centrality," in *2008 Proceedings of the Tenth Workshop on Algorithm Engineering and Experiments (ALENEX)*. SIAM, 2008, pp. 90–100.

[18] V. Gleyzer, A. J. Soszynski, and E. K. Kao, "Leveraging linear algebra to count and enumerate simple subgraphs," in *2020 IEEE High Performance Extreme Computing Conference (HPEC)*. IEEE, 2020, pp. 1–8.

[19] A. Gondimalla, N. Chesnut, M. Thottethodi, and T. Vijaykumar, "Sparten: A sparse tensor accelerator for convolutional neural networks," in *Proceedings of the 52nd Annual IEEE/ACM International Symposium on Microarchitecture*, 2019, pp. 151–165.

[20] J. E. Gonzalez, Y. Low, H. Gu, D. Bickson, and C. Guestrin, "Powergraph: Distributed graph-parallel computation on natural graphs," in *Presented as part of the 10th {USENIX} Symposium on Operating Systems Design and Implementation ({OSDI} 12)*, 2012, pp. 17–30.

[21] K. Hegde, H. Asghari-Moghaddam, M. Pellauer, N. Crago, A. Jaleel, E. Solomonik, J. Emer, and C. W. Fletcher, "Extensor: An accelerator for sparse tensor algebra," in *Proceedings of the 52nd Annual IEEE/ACM International Symposium on Microarchitecture*, 2019, pp. 319–333.

[22] Intel, *Intel 64 and IA-32 Architectures Optimization Reference Manual*, December 2008. [Online]. Available: http://developer.intel.com/products/processor/manuals/

[23] A. P. Iyer, Z. Liu, X. Jin, S. Venkataraman, V. Braverman, and I. Stoica, "{ASAP}: Fast, approximate graph pattern mining at scale," in *13th {USENIX} Symposium on Operating Systems Design and Implementation ({OSDI} 18)*, 2018, pp. 745–761.

[24] K. Jamshidi, R. Mahadasa, and K. Vora, "Peregrine: a pattern-aware graph mining system," in *Proceedings of the Fifteenth European Conference on Computer Systems*, 2020, pp. 1–16.

[25] U. Kang, C. E. Tsourakakis, and C. Faloutsos, "Pegasus: A peta-scale graph mining system implementation and observations," in *2009 Ninth IEEE International Conference on Data Mining*. IEEE, 2009, pp. 229–238.

[26] F. Kjolstad, S. Chou, D. Lugato, S. Kamil, and S. Amarasinghe, "taco: A tool to generate tensor algebra kernels," in *2017 32nd IEEE/ACM International Conference on Automated Software Engineering (ASE)*, Oct 2017, pp. 943–948.

[27] J. M. Kleinberg, "Authoritative sources in a hyperlinked environment," in *Proceedings of the ninth annual ACM-SIAM symposium on Discrete algorithms*, 1998, pp. 668–677.

[28] S. Kumar, F. Spezzano, V. S. Subrahmanian, and C. Faloutsos, "Edge weight prediction in weighted signed networks," in *Proc. Int. Conf. Data Min.*, 2016, pp. 221–230.

[29] J. Kunegis, "Konect: The koblenz network collection," in *Proceedings of the 22nd International Conference on World Wide Web*, ser. WWW '13 Companion. New York, NY, USA: Association for Computing Machinery, 2013, p. 1343–1350. [Online]. Available: https://doi.org/10.1145/2487788.2488173

[30] A. N. Langville and C. D. Meyer, "A reordering for the pagerank problem," *SIAM Journal on Scientific Computing*, vol. 27, no. 6, pp. 2112–2120, 2006.

[31] J. Leskovec, D. Huttenlocher, and J. Kleinberg, "Predicting positive and negative links in online social networks," in *Proceedings of the 19th international conference on World wide web*, 2010, pp. 641–650.

[32] J. Leskovec, D. Huttenlocher, and J. Kleinberg, "Signed networks in social media," in *Proceedings of the SIGCHI conference on human factors in computing systems*, 2010, pp. 1361–1370.

[33] J. Leskovec, J. Kleinberg, and C. Faloutsos, "Graphs over time: densification laws, shrinking diameters and possible explanations," in *Proceedings of the eleventh ACM SIGKDD international conference on Knowledge discovery in data mining*, 2005, pp. 177–187.

[34] J. Leskovec, J. Kleinberg, and C. Faloutsos, "Graph evolution: Densification and shrinking diameters," *ACM transactions on Knowledge Discovery from Data (TKDD)*, vol. 1, no. 1, pp. 2–es, 2007.

[35] J. Leskovec, J. Kleinberg, and C. Faloutsos, "Graph evolution: Densification and shrinking diameters," *ACM transactions on Knowledge Discovery from Data (TKDD)*, vol. 1, no. 1, pp. 2–es, 2007.

[36] J. Leskovec, K. J. Lang, A. Dasgupta, and M. W. Mahoney, "Community structure in large networks: Natural cluster sizes and the absence of large well-defined clusters," *Internet Mathematics*, vol. 6, no. 1, pp. 29–123, 2009.

[37] Y. Low, J. E. Gonzalez, A. Kyrola, D. Bickson, C. E. Guestrin, and J. Hellerstein, "Graphlab: A new framework for parallel machine learning," *arXiv preprint arXiv:1408.2041*, 2014.

[38] G. Malewicz, M. H. Austern, A. J. Bik, J. C. Dehnert, I. Horn, N. Leiser, and G. Czajkowski, "Pregel: a system for large-scale graph processing," in *Proceedings of the 2010 ACM SIGMOD International Conference on Management of data*, 2010, pp. 135–146.

[39] T. Mattson, D. Bader, J. Berry, A. Buluc, J. Dongarra, C. Faloutsos, J. Feo, J. Gilbert, J. Gonzalez, B. Hendrickson *et al.*, "Standards for graph algorithm primitives," in *2013 IEEE High Performance Extreme Computing Conference (HPEC)*. IEEE, 2013, pp. 1–2.

[40] D. Mawhirter, S. Reinehr, C. Holmes, T. Liu, and B. Wu, "Graphzero: Breaking symmetry for efficient graph mining," *arXiv preprint arXiv:1911.12877*, 2019.

[41] D. Mawhirter and B. Wu, "Automine: harmonizing high-level abstraction and high performance for graph mining," in *Proceedings of the 27th ACM Symposium on Operating Systems Principles*, 2019, pp. 509–523.

[42] N. Muralimanohar, R. Balasubramonian, and N. Jouppi, "Cacti 6.0: A tool to model large caches," *HP Laboratories*, 01 2009.

[43] D. Nguyen, A. Lenharth, and K. Pingali, "A lightweight infrastructure for graph analytics," in *Proceedings of the Twenty-Fourth ACM Symposium on Operating Systems Principles*, 2013, pp. 456–471.

[44] M. M. Ozdal, S. Yesil, T. Kim, A. Ayupov, J. Greth, S. Burns, and O. Ozturk, "Energy efficient architecture for graph analytics accelerators," *ACM SIGARCH Computer Architecture News*, vol. 44, no. 3, pp. 166–177, 2016.

[45] X. Qian, B. Sahelices, and J. Torrellas, "Omniorder: Directory-based conflict serialization of transactions," *ACM SIGARCH Computer Architecture News*, vol. 42, no. 3, pp. 421–432, 2014.

[46] S. Rahman, N. Abu-Ghazaleh, and R. Gupta, "Graphpulse: An event-driven hardware accelerator for asynchronous graph processing," in *2020 53rd Annual IEEE/ACM International Symposium on Microarchitecture (MICRO)*. IEEE, 2020, pp. 908–921.

[47] P. Ribeiro, P. Paredes, M. E. Silva, D. Aparicio, and F. Silva, "A survey on subgraph counting: Concepts, algorithms and applications to network motifs and graphlets," *arXiv preprint arXiv:1910.13011*, 2019.

[48] M. Ripeanu, I. Foster, and A. Iamnitchi, "Mapping the gnutella network: Properties of large-scale peer-to-peer systems and implications for system design," *arXiv preprint cs/0209028*, 2002.

[49] R. A. Rossi and N. K. Ahmed, "The network data repository with interactive graph analytics and visualization," in *Proceedings of the Twenty-Ninth AAAI Conference on Artificial Intelligence*, 2015. [Online]. Available: http://networkrepository.com

[50] D. Sanchez and C. Kozyrakis, "Zsim: Fast and accurate microarchitectural simulation of thousand-core systems," in *Proceedings of the 40th Annual International Symposium on Computer Architecture*, ser. ISCA '13. New York, NY, USA: ACM, 2013, pp. 475–486. [Online]. Available: http://doi.acm.org/10.1145/2485922.2485963

[51] D. R. Shaw, "The methods behind the madness: Presidential electoral college strategies, 1988-1996," *The Journal of Politics*, vol. 61, no. 4, pp. 893–913, 1999.

[52] T. Shi, M. Zhai, Y. Xu, and J. Zhai, "Graphpi: High performance graph pattern matching through effective redundancy elimination," in *2020 SC20: International Conference for High Performance Computing, Networking, Storage and Analysis (SC)*. IEEE Computer Society, pp. 1418–1431.

[53] J. Shun and G. E. Blelloch, "Ligra: a lightweight graph processing framework for shared memory," in *Proceedings of the 18th ACM SIGPLAN symposium on Principles and practice of parallel programming*, 2013, pp. 135–146.

[54] S. Smith, J. W. Choi, J. Li, R. Vuduc, J. Park, X. Liu, and G. Karypis. (2017) FROSTT: The formidable repository of open sparse tensors and tools. [Online]. Available: http://frostt.io/

[55] S. Smith and G. Karypis, "Tensor-matrix products with a compressed sparse tensor," in *Proceedings of the 5th Workshop on Irregular Applications: Architectures and Algorithms*, ser. IA¡sup¿3¡/sup¿ '15. New York, NY, USA: Association for Computing Machinery, 2015. [Online]. Available: https://doi.org/10.1145/2833179.2833183

[56] L. Song, Y. Zhuo, X. Qian, H. Li, and Y. Chen, "Graphr: Accelerating graph processing using reram," in *2018 IEEE International Symposium on High Performance Computer Architecture (HPCA)*. IEEE, 2018, pp. 531–543.

[57] C. H. C. Teixeira, A. J. Fonseca, M. Serafini, G. Siganos, M. J. Zaki, and A. Aboulnaga, "Arabesque: A system for distributed graph mining - extended version," *arXiv preprint arXiv:1510.04233*, 2015.

[58] S. Uddin, L. Hossain *et al.*, "Dyad and triad census analysis of crisis communication network," *Social Networking*, vol. 2, no. 01, p. 32, 2013.

[59] K. Wang, Z. Zuo, J. Thorpe, T. Q. Nguyen, and G. H. Xu, "Rstream: marrying relational algebra with streaming for efficient graph mining on a single machine," in *13th {USENIX} Symposium on Operating Systems Design and Implementation ({OSDI} 18)*, 2018, pp. 763–782.

[60] Z. Wang and T. Nowatzki, "Stream-based memory access specialization for general purpose processors," in *2019 ACM/IEEE 46th Annual International Symposium on Computer Architecture (ISCA)*. IEEE, 2019, pp. 736–749.

[61] J. Yang and J. Leskovec, "Defining and evaluating network communities based on ground-truth," *arXiv preprint arXiv:1205.6233*, 2012.

[62] Y. Yang, Z. Li, Y. Deng, Z. Liu, S. Yin, S. Wei, and L. Liu, "Graphabcd: Scaling out graph analytics with asynchronous block coordinate descent," in *2020 ACM/IEEE 47th Annual International Symposium on Computer Architecture (ISCA)*, May 2020, pp. 419–432.

[63] Y. Yang, Z. Li, Y. Deng, Z. Liu, S. Yin, S. Wei, and L. Liu, "Graphabcd: Scaling out graph analytics with asynchronous block coordinate descent," in *2020 ACM/IEEE 47th Annual International Symposium on Computer Architecture (ISCA)*. IEEE, 2020, pp. 419–432.

[64] P. Yao, L. Zheng, Z. Zeng, Y. Huang, C. Gui, X. Liao, H. Jin, and J. Xue, "A locality-aware energy-efficient accelerator for graph mining applications," in *2020 53rd Annual IEEE/ACM International Symposium on Microarchitecture (MICRO)*. IEEE, 2020, pp. 895–907.

[65] H. Yin, A. R. Benson, J. Leskovec, and D. F. Gleich, "Local higher-order graph clustering," in *Proceedings of the 23rd ACM SIGKDD International Conference on Knowledge Discovery and Data Mining*, 2017, pp. 555–564.

[66] M. Zhang, Y. Zhuo, C. Wang, M. Gao, Y. Wu, K. Chen, C. Kozyrakis, and X. Qian, "Graphp: Reducing communication for pim-based graph processing with efficient data partition," in *2018 IEEE International Symposium on High Performance Computer Architecture (HPCA)*. IEEE, 2018, pp. 544–557.

[67] X. Zhu, W. Chen, W. Zheng, and X. Ma, "Gemini: A computation-centric distributed graph processing system," in *12th {USENIX} Symposium on Operating Systems Design and Implementation ({OSDI} 16)*, 2016, pp. 301–316.

[68] Y. Zhuo, C. Wang, M. Zhang, R. Wang, D. Niu, Y. Wang, and X. Qian, "Graphq: Scalable pim-based graph processing," in *Proceedings of the 52nd Annual IEEE/ACM International Symposium on Microarchitecture*, 2019, pp. 712–725.